Hydrothermal Synthesis, Crystal Structure, Solid-State NMR Spectroscopy, and Ionic Conductivity of $Na_5InSi_4O_{12}$, a Silicate Containing a Single 12-Membered Ring

Ling-I Hung,[†] Sue-Lein Wang,[†] Sung-Ping Szu,[‡] Chan-Yen Hsieh,[§] Hsien-Ming Kao,[§] and Kwang-Hwa Lii*[,§,||]

Department of Chemistry, National Tsing Hua University, Hsinchu, Taiwan 300, R.O.C., Department of Physics, National Chung-Hsing University, Taichung, Taiwan 402, R.O.C., Department of Chemistry, National Central University, Chungli, Taiwan 320, R.O.C., and Institute of Chemistry, Academia Sinica, Taipei 115, Taiwan, R.O.C.

Received May 30, 2003. Revised Manuscript Received October 3, 2003

$Na_5InSi_4O_{12}$ has been synthesized by a high-temperature, high-pressure hydrothermal method and characterized by single-crystal X-ray diffraction and solid-state NMR spectroscopy. It is isotypic to $Na_5ScSi_4O_{12}$. The structure consists of 12-membered single rings of corner-sharing SiO_4 tetrahedra linked together via corner sharing by single InO_6 octahedra to form a 3-D framework that delimits two types of channels along the *c*-axis. There are six independent sodium sites. The Na atoms within the 12-ring channels are immobile and the Na atoms within 7-ring channels are highly mobile. The ^{29}Si MAS NMR exhibits one Q^3 and one Q^4 resonance, each of which is split into two peaks because of inequivalent chemical environments caused by partially occupied Na sites in the 7-ring channels. Na ion conductivity measurements on a pressed pellet of the title compound were performed. The Arrhenius plot of dc conductivity shows a change in slope near 220 °C. We attribute this to the activation of the Na site that is situated between 7-ring channels and may serve as a connecting link between the channels. Crystal data: trigonal, space group *R*-3*c* (No. 167), $a = 21.7158(9)$ Å, $c = 12.4479(7)$ Å, and $Z = 18$.

Introduction

Open framework, mixed octahedral and tetrahedral metal oxides have been studied with great intensity because of their interesting structural chemistry and applications in ion exchange and catalysis.[1] A large number of phosphate-based framework structures have been reported.[2−4] Recently much work has focused on the synthesis of metal silicates, because of their generally greater thermal stability than the phosphates. A good number of vanadium silicates have been synthesized.[5−8] Some of them show good thermal stability, absorption, and ion-exchange properties, suggesting their potential for applications as molecular sieves or in catalysis. Their structural chemistry is interesting, as shown by a wide variety of structure types adopted by the compounds with the formula $A_2(VO)Si_4O_{10}\cdot nH_2O$ (A = alkali metals, $n \geq 0$). A series of uranium silicates have also been developed by replacing the VO^{2+} cation in the vanadium(IV) silicates with UO_2^{2+} as the bridging metal species.[9−11] Other recent examples include titanium,[12,13] niobium,[14,15] cerium,[16,17] tin,[18] and indium silicates.[19] Most of these compounds were synthesized under hy-

* Corresponding author. E-mail: liikh@cc.ncu.edu.tw.
[†] National Tsing Hua University.
[‡] National Chung-Hsing University.
[§] National Central University.
[||] Academia Sinica.

(1) Rocha, J.; Anderson, M. W. *Eur. J. Inorg. Chem.* **2000**, 801 and references therein.
(2) Haushalter, R. C.; Mundi, L. A. *Chem. Mater.* **1992**, *4*, 31 and references therein.
(3) Lii, K.-H.; Huang, Y.-F.; Zima, V.; Huang, C.-Y.; Lin, H.-M.; Jiang, Y.-C.; Liao, F.-L.; Wang, S.-L. *Chem. Mater.* **1998**, *10*, 2599 and references therein.
(4) Cheetham, A. K.; Ferey, G.; Loiseau, T. *Angew. Chem., Int. Ed. Engl.* **1999**, *38*, 3268 and references therein.
(5) Wang, X.; Liu, L.; Jacobson, A. J. *Angew. Chem., Int. Ed.* **2001**, *40*, 2174.
(6) Wang, X.; Liu, L.; Jacobson, A. J. *J. Am. Chem. Soc.* **2002**, *124*, 7812.
(7) Huang, J.; Wang, X.; Liu, L.; Jacobson, A. J. *Solid State Sci.* **2002**, *4*, 1193.
(8) Li, C.-Y.; Hsieh, C.-Y.; Lin, H.-M.; Kao, H.-M.; Lii, K.-H. *Inorg. Chem.* **2002**, *41*, 4206.
(9) Wang, X.; Huang, J.; Liu, L.; Jacobson, A. J. *J. Mater. Chem.* **2002**, *12*, 406.
(10) Wang, X.; Huang, J.; Jacobson, A. J. *J. Am. Chem. Soc.* **2002**, *124*, 15190.
(11) Huang, J.; Wang, X.; Jacobson, A. J. *J. Mater. Chem.* **2003**, *13*, 191.
(12) Nyman, M.; Bonhomme, F.; Teter, D. M.; Maxwell, R. S.; Bu, B. X.; Wang, L. M.; Ewing, R. C.; Nenoff, T. M. *Chem. Mater.* **2000**, *12*, 3449.
(13) Nyman, M.; Bonhomme, F.; Maxwell, R. S.; Nenoff, T. M. *Chem. Mater.* **2001**, *13*, 4603.
(14) Francis, R. J.; Jacobson, A. J. *Angew. Chem., Int. Ed.* **2001**, *40*, 2879.
(15) Kao, H.-M.; Lii, K.-H. *Inorg. Chem.* **2002**, *41*, 5644.
(16) Rocha, J.; Ferreira, P.; Carlos, L. D.; Ferreira, A. *Angew. Chem., Int. Ed.* **2000**, *39*, 3276.
(17) Jeong, H.-K.; Chandrasekaran, A.; Tsapatsis, M. *Chem. Commun.* **2002**, 2398.
(18) Ferreira, A.; Lin, Z.; Rocha, J.; Morais, C. M.; Lopes, M.; Fernandez, C. *Inorg. Chem.* **2001**, *40*, 3330.
(19) Hung, L.-I.; Wang, S.-L.; Kao, H.-M.; Lii, K.-H. *Inorg. Chem.* **2003**, *42*, 4057.

10.1021/cm030417e CCC: $27.50
Published on Web 03/19/2004

drothermal conditions at 180−240 °C by using alkali metal cations as templating agents. A uranium and a niobium silicate have been synthesized by using organic templates.[10,14] We have also synthesized a number of new silicates of V, Nb, and In by high-temperature, high-pressure hydrothermal reactions in gold ampules using alkali metal cations as templates.[8,15,19] For example, $Rb_2(VO)Si_4O_{10}{\cdot}xH_2O$, which has the same framework stoichiometry as $K_2(VO)Si_4O_{10}{\cdot}H_2O$ and the mineral $Ca(VO)Si_4O_{10}{\cdot}4H_2O$, adopts a new structure type.[8] We also reported the first example of two-bond *J*-coupling between a quadrupolar nucleus and a spin-1/2 nucleus in the solid state during the NMR study of the new niobium silicate $Rb_4(NbO)_2Si_8O_{21}$.[15] The framework structure of $K_2In(OH)Si_4O_{10}$, which is analogous to that of $K_2CuSi_4O_{10}$, consists of chains of trans-corner-sharing $InO_4(OH)_2$ octahedra and 8-ring channels formed by unbranched vierer 4-fold silicate chains.[19] Both $Cs_2VOSi_6O_{14}$ and $Cs_2VOSi_6O_{14}{\cdot}3H_2O$ contain 8-ring channels, although the former was prepared under much more vigorous hydrothermal conditions than the latter.[20] In this paper, we report an indium silicate, $Na_5InSi_4O_{12}$ (**1**), which contains 12-membered single rings of silicate tetrahedra. The solid-state NMR spectroscopy and ionic conductivity have also been studied.

Experimental Section

Synthesis and Initial Characterization. The hydrothermal reactions were carried out under autogenous pressure in gold ampules contained in a Leco Tem-Pres autoclave, where pressure was provided by water. The degree of filling of the autoclave by water at room temperature was 55%. All chemicals were purchased from Aldrich Chemicals. A reaction mixture of NaOH(aq), In_2O_3, and SiO_2 (molar ratio Na:In:Si = 10:1:4) in a 6.5 cm long gold ampule (inside diameter = 4.85 mm) was heated at 600 °C for 3 d. The pressure was estimated to be 170 MPa according to the pressure−temperature diagram of pure water. The autoclave was then cooled to 350 °C at 5 °C/h followed by fast cooling to room temperature by turning off the power of the tube furnace. The product contained colorless rod crystal and powder. A crystal was selected for structure determination by single-crystal X-ray diffraction. Powder X-ray data were collected on a Shimadzu XRD-6000 automated powder diffractometer with Cu Kα radiation equipped with a scintillation detector. Data were collected in the range $5° \le 2\theta \le 50°$ using $\theta-2\theta$ mode in a flat-plate geometry. The bulk product was a single phase of $Na_5InSi_4O_{12}$, **1**, because its powder pattern is in good agreement with the calculated pattern based on the results from single-crystal X-ray diffraction (Figure 1). The program XPOW in the SHELXTL version 5.1 software package was used for XRPD simulation.[21] The yield was 82% based on indium. The sample was used for ionic conductivity and solid-state NMR studies. Reaction of NaOH(aq), V_2O_3, and SiO_2 (molar ratio Na:V:Si = 4:1:4) for 3 d at 550 °C followed by slow cooling at 5 °C/h to 275 °C produced $Na_5VSi_4O_{12}$ as green rod crystals in a low yield. $Na_5VSi_4O_{12}$ is isotypic to **1**.[22]

A powder sample of **1** was stirred at 70 °C for 12 h in a 100-fold excess, 2 M aqueous solution of lithium nitrate and then washed with water and ethanol. An X-ray powder pattern of the sample was measured and compared with the pattern before ion exchange. The agreement between the two patterns

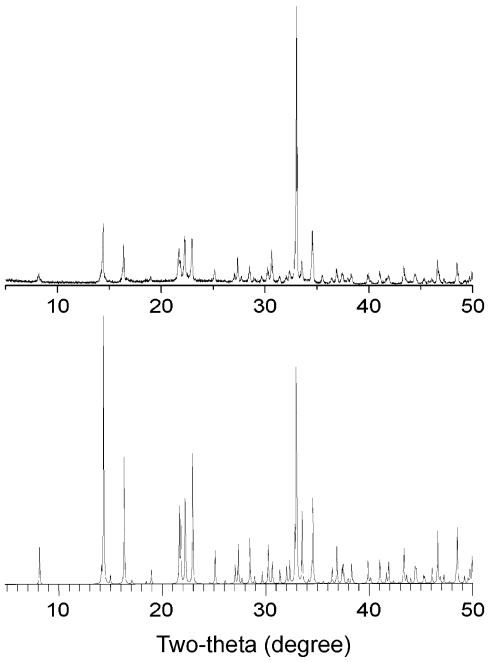

Figure 1. (a) X-ray powder pattern of $Na_5InSi_4O_{12}$. (b) Simulated powder pattern from the atomic coordinates derived from single-crystal X-ray diffraction.

is generally good with respect to the relative peak intensity and the peak positions of strong reflections, though all peaks are considerably broadened after ion exchange. Elemental analysis of the sample by ICP shows that the indium content remains essentially the same and 80% of Na^+ ions are exchanged by Li^+. However, the total amount of Na^+ and Li^+ ions is only 70% of that before ion exchange. These studies show that the chemical durability of **1** in concentrated aqueous solution of $LiNO_3$ at 70 °C is poor. There is loss of Na and silicate due to leaching.

Single-Crystal X-ray Diffraction. A suitable crystal of **1** was selected for indexing and intensity data collection on a Siemens SMART CCD diffractometer equipped with a normal focus, 3-kW sealed tube X-ray source. Intensity data were collected at room temperature in 1271 frames with ω scans (width 0.30° per frame). Empirical absorption corrections based on symmetry equivalents were applied. On the basis of reflection conditions, statistical analysis of the intensity distributions, and successful solution and refinement of the structures, the space group was determined to be *R*-3*c* (No. 167). The structure was solved by direct methods and difference Fourier syntheses. The In atom was located at 18e special position with a local symmetry of C_2, and all Si and O atoms at general positions. Six Na sites were located. Na(1) and Na(3) were located at 36f general positions, Na(2) at 18e, Na(4) at 18d, Na(5) at 6b, and Na(6) at 6a special positions. We earlier refined the structures with all Na sites fully occupied. Both Na(3) and Na(4) atoms showed very large thermal parameters, which are indicative of partial occupancy or positional disorder. The Na(3)···Na(4) distance is very short (1.596(5) Å), precluding simultaneous Na occupancy of these two sites. The multiplicities of both Na atoms were allowed to refine. The Na(3) and Na(4) positions respectively refined to multiplicities of 0.31(1) and 0.322(9), indicating that Na(3) and Na(4) sites are one-third and two-thirds occupied, respectively. The final cycles of least-squares refinement including atomic coordinates, anisotropic thermal parameters for all atoms, and fixed multiplicities for partially occupied Na positions converged at R1 = 0.0446 and wR2 = 0.0841. The final difference electron density maps were featureless and the highest peak and deepest hole were 0.66 and −0.65 e/Å^3. All calculations were performed using SHELXTL Version 5.1 software package. The crystal data and structure refinement parameters are

(20) Huang, L.-I.; Wang, S.-L.; Lii, K.-H. Unpublished research.
(21) Sheldrick, G. M. *SHELXTL Programs*, version 5.1; Bruker AXS GmbH: Karlsruhe, Germany, 1998.
(22) $Na_5VSi_4O_{12}$ is characterized by single-crystal X-ray diffraction. Crystal data: trigonal, space group *R*-3*c* (No. 167), $a = 21.4004(5)$ Å, $c = 12.3665(6)$ Å, $V = 4904.8(3)$ Å^3, $Z = 18$, R1 = 0.0229, and wR2 = 0.0607.

Table 1. Crystallographic Data for $Na_5InSi_4O_{12}$

chemical formula	$InNa_5O_{12}Si_4$
crystal system	trigonal
space group	*R*3*c* (No. 167)
a/Å	21.7158(9)
c/Å	12.4479(7)
V/Å^3	5083.7(4)
Z	18
formula weight	534.13
T, °C	23
λ(Mo Kα), Å	0.71073
D_{calc}, g·cm^{-3}	3.140
μ(Mo Kα), cm^{-1}	27.8
unique data ($I > 2\sigma(I)$)	1363
no. of variables	112
R1[a]	0.0446
wR2[b]	0.0841
$(\Delta\rho)_{max,min}$	0.66, −0.65

[a] $R1 = \sum||F_o| - |F_c||/\sum|F_o|$. [b] $wR2 = [\sum w(F_o^2 - F_c^2)^2/\sum w(F_o^2)^2]^{1/2}$, $w = 1/[\sigma^2(F_o^2) + (aP)^2 + bP]$, $P = [\max(F_o,0) + 2(F_c)^2]/3$, where $a = 0$ and $b = 87.11$.

Table 2. Atomic Coordinates and Thermal Parameters for $Na_5InSi_4O_{12}$

atom	position	occupancy	x	y	z	U_{eq}[a]
Na(1)	36f	1	0.5932(1)	0.1926(1)	−0.0298(2)	0.0191(5)
Na(2)	18e	1	1/3	−0.0528(2)	−1/12	0.0251(8)
Na(3)	36f	1/3	0.3287(5)	0.1810(5)	0.044(1)	0.057(3)
Na(4)	18d	2/3	1/3	1/6	1/6	0.053(2)
Na(5)	6b	1	2/3	1/3	−1/6	0.017(1)
Na(6)	6a	1	2/3	1/3	1/12	0.017(1)
In(1)	18e	1	0.41918(2)	0.08585(2)	1/12	0.0086(2)
Si(1)	36f	1	0.42941(8)	0.11310(8)	−0.1866(1)	0.0095(3)
Si(2)	36f	1	0.48251(7)	0.24390(8)	−0.0423(1)	0.0094(3)
O(1)	36f	1	0.3557(2)	0.0831(2)	−0.2484(3)	0.0165(8)
O(2)	36f	1	0.4312(2)	0.0696(2)	−0.0847(3)	0.0151(8)
O(3)	36f	1	0.4851(2)	0.1168(2)	−0.2806(3)	0.0155(8)
O(4)	36f	1	0.4573(2)	0.1966(2)	−0.1542(3)	0.0179(9)
O(5)	36f	1	0.4447(2)	0.1945(2)	0.0607(3)	0.0144(8)
O(6)	36f	1	0.5671(2)	0.2866(2)	−0.0366(3)	0.0173(8)

[a] U_{eq} is defined as one-third of the trace of the orthogonalized U_{ij} tensor.

Table 3. Bond Lengths (Å) for $Na_5InSi_4O_{12}$

Na(1)−O(5)	2.340(5)	Na(1)−O(6)	2.341(5)
Na(1)−O(6)	2.378(5)	Na(1)−O(4)	2.388(5)
Na(1)−O(3)	2.916(5)	Na(1)−O(6)	3.005(5)
Na(2)−O(1)	2.386(4) (2×)	Na(2)−O(2)	2.437(5) (2×)
Na(2)−O(3)	2.537(5)	Na(3)−O(2)	2.30(1)
Na(3)−O(5)	2.40(1)	Na(3)−O(1)	2.49(1)
Na(3)−O(4)	2.58(1)	Na(3)−O(3)	2.86(1)
Na(4)−O(1)	2.351(4) (2×)	Na(4)−O(5)	2.548(4) (2×)
Na(4)−O(2)	2.809(4) (2×)	Na(5)−O(6)	2.476(4) (6×)
Na(6)−O(6)	2.395(4) (6×)	In(1)−O(1)	2.131(4) (2×)
In(1)−O(5)	2.156(4) (2×)	In(1)−O(2)	2.159(4) (2×)
Si(1)−O(1)	1.592(4)	Si(1)−O(2)	1.593(4)
Si(1)−O(3)	1.648(4)	Si(1)−O(4)	1.656(4)
Si(2)−O(3)	1.655(4)	Si(2)−O(4)	1.653(4)
Si(2)−O(5)	1.609(4)	Si(2)−O(6)	1.593(4)

given in Table 1, the atomic coordinates are in Table 2, and selected bond distances are in Table 3.

Solid-State NMR Measurements. ^{29}Si magic angle spinning (MAS) NMR spectra were recorded on a Bruker AVANCE-400 spectrometer equipped with a double-tuned 4 mm MAS probe, with a resonance frequency of 79.46 MHz for ^{29}Si nucleus. A pulse length of 2 μs (π/6 pulse) and a repetition time of 20 s were used to obtain ^{29}Si MAS NMR spectra. T_1 values of about 20 s for all the ^{29}Si resonances were obtained with an inversion−recovery pulse sequence. ^{29}Si chemical shifts were externally referenced to tetramethylsilane (TMS) at 0 ppm. ^{23}Na MAS NMR spectra at 293 K and several temperatures up to 473 K were also recorded. The spectra are complex with overlapping line shapes. We are unable to provide a reasonable interpretation of the spectra at present.

Ionic Conductivity Measurements. A pellet with a thickness of 0.1 cm and a diameter of 0.6 cm was prepared by pressing a powder sample of **1** in a die. The pellet was annealed at 550 °C in air for 5 h in order to minimize the grain boundary effect. For better contact, gold was coated on both sides of the pellet by thermal evaporation method. The ac-complex impedance was measured using a HP4194A impedance analyzer. A frequency range from 100 Hz to 15 MHz was employed. Measurements were made in flowing nitrogen gas over a temperature range from 30 to 500 °C at a heating rate of 2 °C/min.

Results and Discussion

Structure. As shown in Figure 2, the structure of **1** is constructed from the following structural elements: two SiO_4 tetrahedra at general positions, one InO_6 octahedron with a local symmetry of C_2, and six Na sites. Si(1)O_4 is bonded to two Si(2)O_4 tetrahedra and two InO_6 octahedra. Si(2)O_4 is bonded to two Si(1)O_4 tetrahedra and one InO_6 octahedron with one terminal oxygen, O(6). Both Na(3) and Na(4) sites are partially occupied with a multiplicity of 0.33, and all other Na sites are fully occupied. The structure consists of 12-membered, puckered, single rings of corner-sharing SiO_4 tetrahedra in the *ab*-plane linked together via corner sharing by single InO_6 octahedra to form a 3-D framework that delimits two types of channels along the *c*-axis. Channels of the first type are formed by stacking the 12-membered rings. In the cores of the 12-ring channels are 6-coordinate Na(5) and Na(6) atoms. These two Na atoms are tightly bonded in the channels and probably immobile, as indicated by short and regular Na−O bond lengths and nearly isotropic thermal vibrations. Channels of the second type are located between neighboring 12-ring channels and contain 7-membered rings, which are formed by the edges of two octahedra and five tetrahedra. Na(3) and Na(4) sites are situated in 7-ring channels (Figure 3a). The Na(3)···Na(4) distance is very short (1.596(5) Å), precluding simultaneous Na occupancy of these two sites. The minimum O···O distance across the 7-ring less one oxygen diameter of 2.76 Å is 1.94 Å, which is slightly smaller than the diameter of 6-coordinate Na^+ ion (2.04 Å).[23] On the basis of the temperature factors of the oxygen atoms ($U_{eq} \sim 0.015$ Å^2), their root-mean-square vibrational amplitudes are around 0.12 Å. Therefore, the thermal vibrations of the oxygen atoms would make the window just large enough at room temperature for Na^+ ions to pass through. The partial occupancy of these two sites and large anisotropic thermal parameters [$U_{33} \sim 8U_{11} \sim 4U_{22}$ for Na(3) and $U_{33} \sim 3U_{11} \sim 6U_{22}$ for Na(4)] all imply that these two Na atoms are highly mobile. Na(1) is probably immobile because of small and nearly isotropic thermal vibrations. Na(2) is situated between 7-ring channels with some anisotropy of thermal vibrations ($U_{11} \sim 1.5U_{22} \sim 3U_{33}$). To migrate from the Na(2) site to the Na(3) or Na(4) site, a Na^+ ion has to pass through a triangular window formed by three oxygen atoms (Figure 3b). The three edge lengths of the triangle are 4.21, 3.94, and 2.74 Å, and the distances from the centroid to the three oxygen atoms are 2.56, 1.97, and 1.78 Å. Migration of Na^+ from the Na(2) site to the Na(3) or Na(4) site is difficult and is associated with an

(23) Shannon, R. D. *Acta Crystallogr.* **1976**, *A32*, 751.

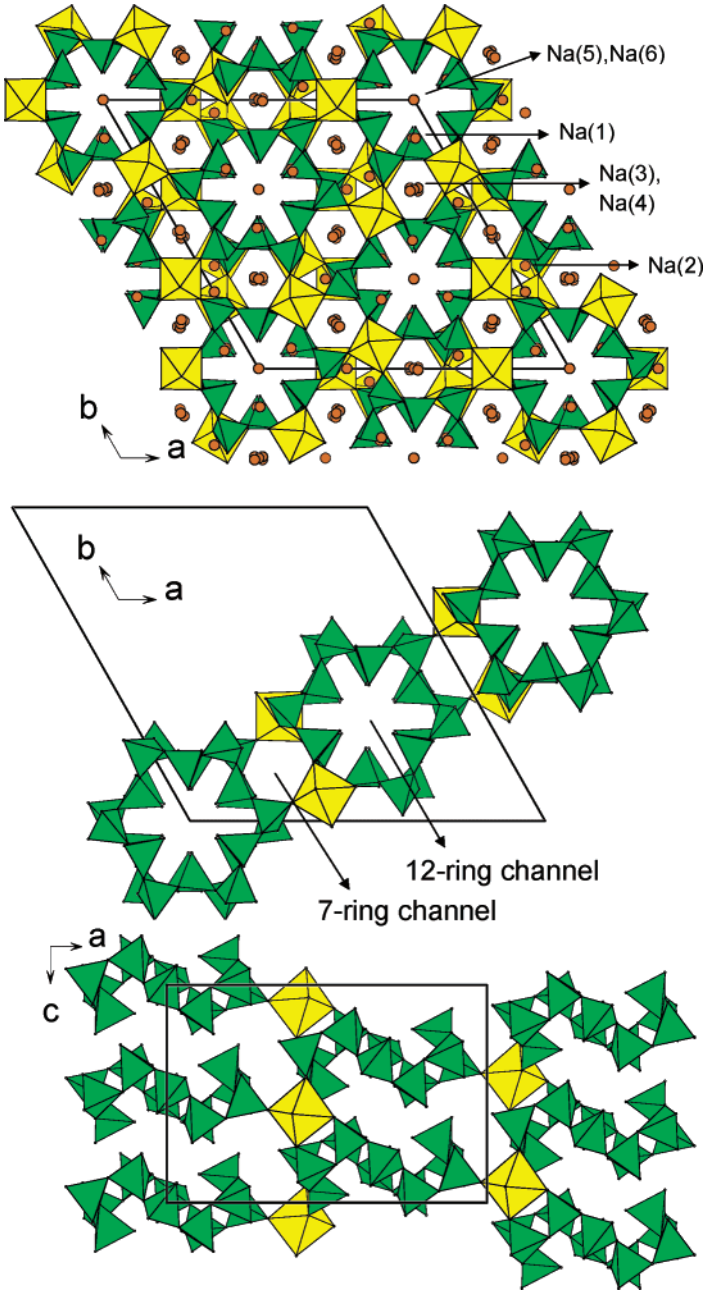

Figure 2. (a) Structure of $Na_5InSi_4O_{12}$ viewed along the *c* axis. The yellow and green polyhedra are InO_6 octahedra and SiO_4 tetrahedra, respectively. Orange circles are sodium atoms. (b) Section of the structure showing the 12-ring and 7-ring channels and the connectivity between the silicate rings and InO_6 octahedra.

activation energy barrier at room temperature. However, a Na^+ ion would be able to squeeze through the triangular window at high temperature. The Na(2) site may serve as connecting links between the channels containing Na(3) and Na(4) sites, as suggested by Shannon et al.[24]

Compound **1** is isotypic to $Na_5ScSi_4O_{10}$, which was also synthesized under hydrothermal conditions.[25] However, the Na atom at the 18d special position with an occupancy factor of 2/3 in the structural refinement of compound **1** was located at 36f general position with an occupancy factor of 1/3 in the refinement of the Sc silicate. Shannon et al. reported ionic conductivity in a series of $Na_5YSi_4O_{12}$-type silicates.[24] Most of the compositions studied were rare earth silicates. The indium compound was also prepared, but its crystal structure and ionic conductivity were not reported.

Solid-State NMR Spectroscopy. The local environment of the SiO_4 unit is sensitively reflected in the chemical shift of the central Si atom. Characteristic high-field shifts (i.e. more negative δ values) are observed with increasing degree of SiO_4 polymerization. In aluminosilicates, the replacement of one or more Si atoms by Al atoms results in significant low-field shifts. The ^{29}Si one-pulse MAS NMR spectrum of **1** is shown in Figure 4. Four resonances, which can be divided into two groups at (−83.7, −82.8) and (−78.8, −78.4) ppm, are observed with approximately equal intensities. Si-

(24) Shannon, R. D.; Taylor, B. E.; Gier, T. E.; Chen, H.-Y.; Berzins, T. *Inorg. Chem.* **1978**, *17*, 958.
(25) Merinov, B. V.; Maksimov, B. A.; Belov, N. V. *Sov. Phys. Dokl.* **1980**, *25*, 885.

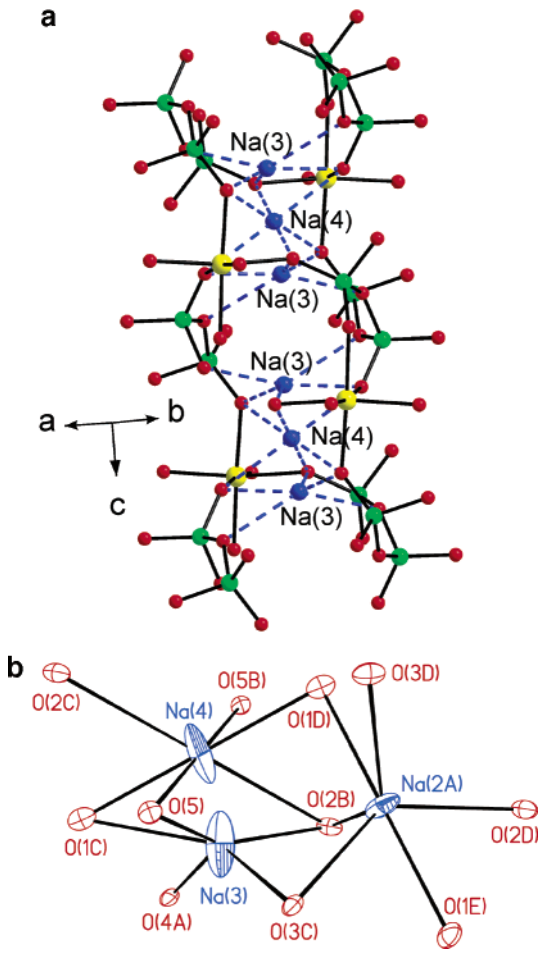

Figure 3. (a) Section of a 7-ring channel in the structure of $Na_5InSi_4O_{12}$ viewed in a perpendicular direction showing the coordination environments of the partially occupied Na sites. (b) Coordination environments of Na atoms showing the connectivity between the Na(2) site and partially occupied Na sites.

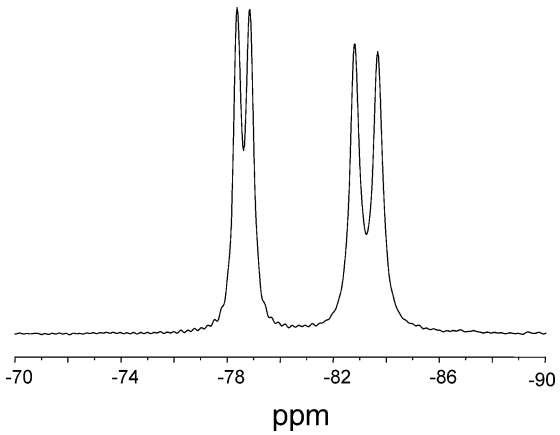

Figure 4. ^{29}Si one-pulse NMR spectrum of $Na_5InSi_4O_{12}$ acquired at a spinning speed of 8 kHz.

(1) is a Q^4(2 In) unit, whereas Si(2) is a Q^3(1 In) unit. The chemical shifts of Q^4(2 Al) and Q^3(1 Al) units in aluminosilicates are in the ranges from −92 to −100 ppm and −84 to −91 ppm, respectively.[26] The group of resonances with low-field shifts in Figure 4 is therefore assigned to Si(2) and the other group to Si(1). The splitting of each Si resonance into two peaks of equal intensity can be considered to be related to the partially occupied Na(3) and Na(4) sites with equal number of Na atoms in a unit cell. The very short distance between the two Na sites precludes simultaneous occupancy, which gives rise to two slightly different chemical environments for both Si atoms. The splitting of Si(1) is larger because all four oxygen atoms in $Si(1)O_4$ are coordinated to Na(3) and Na(4) as compared to only three oxygen atoms for $Si(2)O_4$. $K_2In(OH)Si_4O_{10}$ displays high-field shifts (from −88 to −98 ppm) as compared to **1**, because all four Si atoms in the former are Q^4(1 In) units.[19]

Ionic Conductivity. There are several formalisms that may be used to represent and analyze the impedance measurement results. Various types of information are obtained from the different formalisms. Figure 5a shows the complex impedance $Z'-Z''$ plot for the sample measured at 120 °C. The dc resistance is the intercept of the semicircle with the Z' axis of the complex plot. The departure of the semicircle in the low-frequency part is due to an electrode effect.[27] Figure 5b shows the plot of the variations of the real part conductivity as a function of frequency. As frequency increases, there are three kinds of contribution to the conductivity. They are bulk conductivity, grain boundary conductivity, and electrode effects.[28]

Apart from the impedance representation discussed above, the electric modulus is also a useful representation for the ac impedance measurement. The complex electric modulus M^* is related to the complex impedance by $M^* = j\omega C_o Z^*$, where C_o is the geometric capacitance of the specimen and ω is the angular frequency. The imaginary part of the electric modulus as a function of frequency at 120 °C is shown in Figure 5c, which clearly shows a shoulder and a peak. The positions of the shoulder and the peak are around 10^5 and 10^7 Hz, respectively. The shoulder at lower frequency is due to the relaxation process for sodium ions crossing the grain boundary. The peak at high frequency is due to the relaxation process for sodium ions hopping within the bulk. It is still observed even at room temperature. On the basis of the results from the structural study, the bulk conductivity at high frequency may be ascribed to the highly mobile Na ions at the Na(3) and Na(4) sites in the smaller channels.

Figure 6 is the Arrhenius plot of the dc conductivities (grain boundary conductivity). The conductivities can be separated into two groups, in addition to the decrease of conductivity at low temperature that is due to the loss of physically absorbed water. The activation energies at low- and high-temperature regions are $E_L = 0.45$ eV and $E_H = 0.60$ eV, respectively. The change of activation at high temperature can be ascribed to the activation of sodium at the Na(2) site, which may serve as connecting links between the channels containing Na(3) and Na(4) sites. Na(2) is less mobile than Na(3) and Na(4); hence, the former has higher activation energy.

(26) Engelhardt, G.; Koller, H. In *Solid-State NMR II, Inorganic Matter*; Blümich, B., Ed.; Springer-Verlag: Berlin 1994; pp 3−29.

(27) Villegas, M. A.; Jurado, L. R.; Fernandez Navarro, J. M. *J. Mater. Sci.* **1989**, *24*, 2884.

(28) Odile, B.; Joël, E.; Jean-Louis, F. *Solid State Ionics* **2003**, *158*, 119.

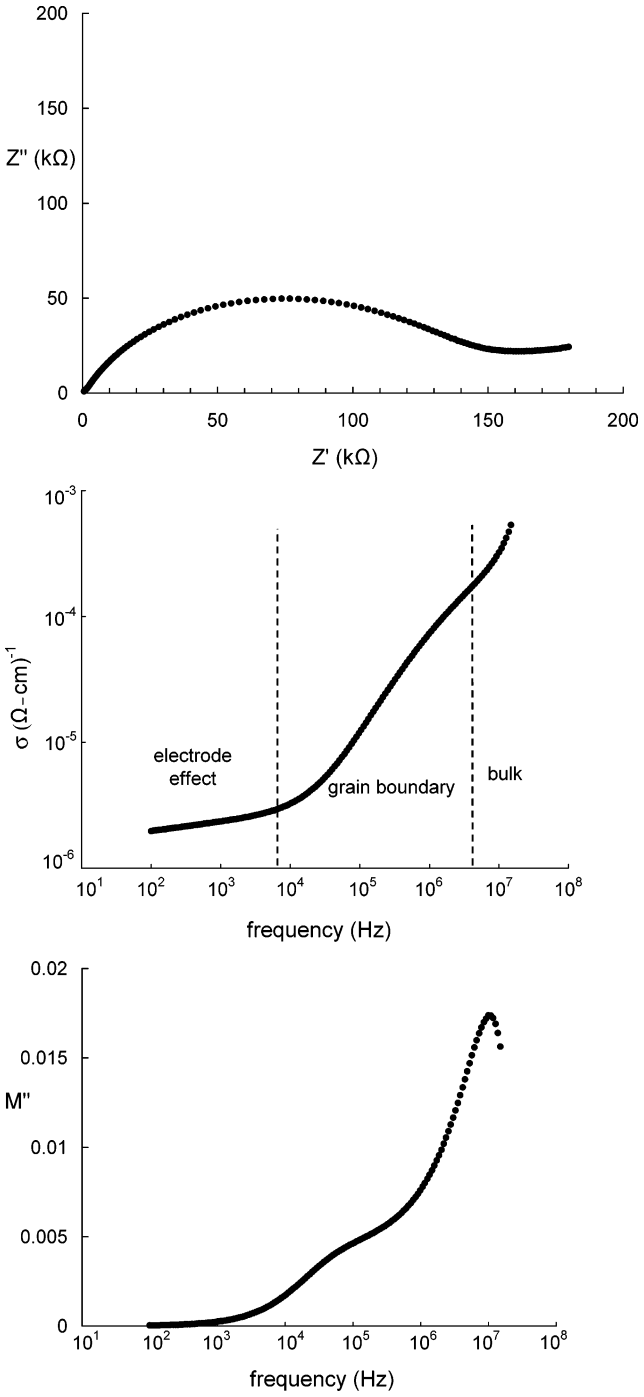

Figure 5. (a) Plots of the $Z'-Z''$ complex impedance spectrum measured at 120 °C on a pressed pellet of $Na_5InSi_4O_{12}$, (b) the real part of the conductivity, and (c) the imaginary part of the electrical modulus as a function of frequency.

Since the activation energies in Figure 6 are obtained from grain boundary conductivity, these activation energies are the sum of energy for sodium hopping between partially occupied sites and the energy for sodium migrating through the grain boundary. If the energy barriers for sodium crossing the grain boundary and hopping between Na(3) and Na(4) sites do not change with temperature, the hopping energy between Na(2) and Na(3) sites is equal to the difference of the two activation energies, which is 0.15 eV. This is a reasonable value for cation migration between vacancies, which can be compared with the activation energy

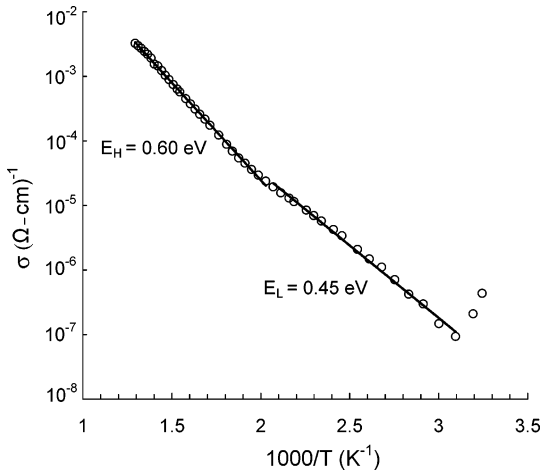

Figure 6. The Arrhenius plot of conductivity versus inverse temperature for $Na_5InSi_4O_{12}$.

for Na^+ β-alumina (0.16 eV) and the migration energy of cation vacancy in AgCl (0.27−0.34 eV).[29,30]

Shannon et al. reported that Na ion conductivities in $Na_5YSi_4O_{12}$-type silicates are proportional to the size of the M^{3+} ion.[24] The Arrhenius plots of the dc conductivities for $Na_5MSi_4O_{12}$ (M = Fe, Sc, and the rare earths) in the range from room temperature to 500 K were shown. The largest rare earths ions give the highest conductivity. The smallest Fe^{3+} ion shows the lowest conductivity. The conductivity for $Na_5InSi_4O_{12}$ was not reported. Our study shows that the conductivity for **1** is considerably lower than that for $Na_5ScSi_4O_{12}$, although the size of M^{3+} and the unit cell volume for the former are significantly larger than the latter. Shannon et al. noted that the $\sigma-1/T$ plots frequently showed a change in slope at 120−180 °C and attributed this to a second phase of lower conductivity at the grain boundary.

Concluding Remarks. We have synthesized an indium(III) silicate and characterized its structure by single-crystal X-ray diffraction and solid-state NMR spectroscopy. The structure consists of 12-membered single rings linked by single octahedra to form a 3-D framework containing 12-ring and 7-ring channels. Highly mobile Na atoms are situated in the 7-ring channels. The ^{29}Si MAS NMR spectrum shows Q^3 and Q^4 peaks, where the splitting of each peak into two lines is related to the partially occupied Na sites. A change in slope near 220 °C in the Arrhenius plot of dc conductivity can be ascribed to the activation of the Na site, which is situated between 7-ring channels. The chemical durability of the title compound in a concentrated aqueous solution of $LiNO_3$ at 70 °C is poor.

A large number of metal silicates have been prepared under mild hydrothermal conditions at 180−240 °C. Their structures are considerably different from those silicates prepared under high-temperature (>500 °C), high-pressure hydrothermal conditions, even though they have identical framework stoichiometry. All metal silicates prepared under high-*T*, high-*P* hydrothermal

(29) Whittingham, M. S.; Huggins, R. A. *Solid State Chemistry*, NBS special publication 364, **1972**, 139.
(30) West, A. R. *Solid State Chemistry and Its Applications*; John Wiley and Sons: New York, 1984; Chapter 13.

conditions by us are anhydrous compounds. In contrast, most metal silicates prepared under mild hydrothermal conditions contain lattice water molecules in the structural channels. The structural chemistry of metal silicates appears to be very rich. Given the large variety of organic templates and inorganic cations that could be used in the hydrothermal synthesis, the scope for the synthesis of further novel compounds in the system of metal silicates appears to be very large.

Acknowledgment. The authors thank the National Science Council for support and Ms. R.-R. Wu at National Cheng Kung University for NMR measurements.

Supporting Information Available: Crystallographic data for $Na_5InSi_4O_{12}$ in CIF format. This material is available free of charge via the Internet at http://pubs.acs.org.

CM030417E